Chapter III

Depletion of ZBP-89 in the intestinal epithelium results in alterations in both secretory and absorptive cell lineages

Summary

ZBP-89 (ZNF148, Zfp148) is a Kruppel-type transcription factor ubiquitously expressed in humans and mice. *In vitro* studies using a number of colorectal and gastric cancer cell lines have shown an increase in ZBP-89 mRNA, suggesting a role for this factor in cancers of the gastrointestinal tract. In fact, recent results suggest that ZBP-89 might normally function as a tumor suppressor and might be used as a marker for transformation in cancer screening. ZBP-89 is also known to play roles in cellular proliferation, differentiation, growth arrest and apoptosis so this association with cancer is not unexpected. The exact function of ZBP-89 in these processes has yet to be tested in an *in vivo* model; therefore in this study, we generated mice deficient in ZBP-89 in the intestine. Mice harboring loxP sites upstream of exon8 and downstream of exon9 of the ZBP-89 gene were bred to mice expressing Cre recombinase from the villin promoter. Conditional loss of ZBP-89 in the intestine results in no gross abnormalities other than a propensity for reduced body weight. Upon histological analysis, homozygous floxed mice displayed higher numbers of goblet and Paneth cells in the secretory lineage as well as almost complete loss of the absorptive cell lineage. These results suggest that loss of ZBP-89 affects normal cell proliferation and differentiation in the intestine.

Introduction

During gastrulation, the epithelium of the mouse small intestine is derived from endoderm and forms a stratified cuboidal epithelium that persists until mid-gestation (11). Regional patterning along the anterior-posterior axis of the gut is established through epithelial-mesenchymal interactions and occurs during middle to late gestation (19, 20, 24). Through these interactions signals from the mesenchyme induce remodeling of the epithelium to form a single layer of columnar cells and to evaginate forming villi by 14 days post coitum (dpc). The fetal villi consist of 3 types of mature epithelial cells: enterocytes which function to absorb nutrients, enteroendocrine cells that release hormones and goblet cells which secrete a protective mucous barrier (26). Also formed are intervillus regions which will eventually invaginate into the mucosa in the days following birth to form crypts (9). After birth, Paneth cells which secrete antibacterial peptides occupy the base of the crypts. Intestinal stem cells are thought to reside in the crypts and as newly differentiated cells are produced they migrate up the villi and then undergo apoptosis at the villus tip, or in the case of Paneth cells migration is downward into the crypt base (5). The entire villus epithelium turns over every three to five days in the mouse and is balanced by the rapid rate of cell proliferation from the stem cells located in the crypts (5). The Wnt and Hedgehog signaling pathways are thought to play a role in this complex morphogenetic process however the exact mechanisms by which this is accomplished remain elusive (14, 24, 27, 41).

Though the exact mechanisms by which cell patterning in the intestine occur remain vague, what is clear is that alteration to normal cellular proliferation and

differentiation in the gastrointestinal tract contribute to a range of disease states in both mice and humans. For example, loss of the absorptive enterocyte leads to malabsorption, a mechanism underlying malnutrition and growth retardation (31). In addition, alterations in epithelial function have been linked to the pathogenesis of chronic inflammation in the intestine. Specifically Crohn's disease is characterized by cycles of ulceration and mucosal injury with inflammation followed by periods of epithelial regeneration and restoration of normal epithelial function (46). In human inflammatory bowel disease (IBD), pathology has shown expansion of the proliferative zone, increased crypt branching, and changes in the normal patterns of differentiation (46). These observations suggest the regulatory pathways that govern proliferation and differentiation are altered in certain diseases of the gastrointestinal tract. Therefore understanding the regulatory pathways active in the gastrointestinal tract as well as the pathological outcomes of altering these pathways will bring clarity to disease etiology.

Villin, a cytoskeletal protein found in the apical brush border of absorptive tissues, is thought to be chiefly disseminated in the villi of intestinal and renal proximal tubular epithelia (15, 39). This protein can be detected as early as 9.0 dpc in the intestinal hindgut endoderm of the mouse and is thus one of the first transcriptionally activated structural genes in the embryonic intestine (9, 28). At 10 dpc, villin expression broadens to include the distal stomach as well as large and small intestinal endoderm (9, 30). By embryonic day 16, villin expression is confined to the intestine and neighboring cells of the stomach now display extremely low levels of villin (9). After birth when the crypts are formed villin expression extends

into these invaginations (30). At this point villin is expressed in all epithelial cells along the crypt-villus axis (28). However, villin is not expressed in the smooth muscle or mesenchyme. A 12.4 kb region of the mouse villin gene has been shown to drive both β-galactosidase and Cre recombinase gene expression in a pattern that mimics the normal villin expression pattern in the intestine (28). Thus villin-cre expressing transgenic mice can be utilized to delete genes in the epithelial mucosa with loxP Cre recombinase recognition sites.

Here we utilized the villin-cre mouse line to delete the transcription factor ZBP-89 from the mouse intestinal epithelium. ZBP-89 (ZNF148, Zfp148) is a ubiquitously expressed multifunctional transcription factor associated with signaling pathways upstream of genes involved in embryogenesis, cellular proliferation, differentiation, growth arrest and apoptosis (2, 23, 32, 43, 49). Furthermore ZBP-89 contains bifunctional regulatory domains that mediate both activator and repressor functions of the transcription factor (16, 35). It is known to exert its effects through both direct binding to GC-rich promoter elements as well as protein-protein interactions (3, 23, 32). A few of the proteins ZBP-89 is known to interact with are Sp1, $p21^{waf1}$, p53, the co-activator p300, Gata-1, Friend of Gata-1 (FOG-1), Sox14, Sox18, and ataxia-telangiectasia mutated (ATM) (1-3, 12, 36, 48, 49, 51). These interactions were demonstrated in *in vitro* systems, but their roles in an *in vivo* model have yet to be examined.

Therefore, we generated a mouse model to study the effects of a ZBP-89 null phenotype in the intestine. This organ was chosen due to a potential role of ZBP-89 in intestinal cell function and cancers of the gastrointestinal tract (1, 4, 21, 33, 44).

Although mouse models of ZBP-89 have been generated by us and others, none of the models successfully represent a null phenotype. Intestinal overexpression of ZBP-89 has been shown to activate apoptosis and mitigate disease burden in $Apc^{Min/+}$ mice (22). Alternatively, knock-in mice devoid of the amino-terminal 127 residues of ZBP-89 protein experience reduced viability, growth delay, and increased susceptibility to dextran sodium sulfate (DSS) induced colitis (21). In an effort to generate mice completely null for ZBP-89, Takeuchi and colleagues showed that mice heterozygous for the null ZBP-89 allele are not compatible with male germ cell development resulting in infertile chimeras (43). In addition to this observation Li and colleagues showed that a ZBP-89 knock-down in zebrafish disrupts hematopoiesis resulting in a bloodless phenotype (25).

In an effort to bypass complications from a complete ZBP-89 null locus we generated mice with loxP sites flanking exons 8 and 9 of the ZBP-89 gene. Upon breeding these mice with those expressing the villin-cre transgene, we effectively deleted ZBP-89 from the intestinal epithelium. We observed widespread induction of both goblet and Paneth cell populations, and a reduced number of enterocytes. Surprisingly expansion of these secretory lineages did not affect enteroendocrine cell numbers, the other member of the secretory lineage in this tissue, suggesting that loss of ZBP-89 affects pathways downstream of the common secretory progenitor from which all three secretory lineages arise.

Materials and Methods

Mice

ZBP-89$^{FLP/FLP}$ mice were generated by insertion of a loxP site and neomycin resistance cassette into intron 7 and insertion of a second loxP site downstream of exon 9 in the ZBP-89 gene. Following germline transmission of the targeted allele, the mice were crossed to FLPe expressing mice to delete the neomycin cassette. Villin-cre mice express CRE recombinase under the control of a 12.4 kb portion of the mouse villin promoter throughout the intestinal epithelium and were a gift from D. Gumucio (The University of Michigan, Ann Arbor, MI) (28). ZBP-89$^{FLP/+}$ mice and villin-cre mice were backcrossed to generate villin-cre/ZBP-89$^{FLP/FLP}$ mice. Genotyping was performed by PCR amplification of tail DNA with specific primers for each gene (5' to 3') were ZBP89-5124F: AGA CCT ACG ACC CAC AGG GTG G and ZBP89-7050R: GGC TTC TCT CCA CTG TGA GTT for the ZBP-89 FLP/FLP; CreORFREV2: GTT CTT GCG AAC CTC ATC C, MVP5498F: ACA GGC ACT AAG GGA GCC AAT G and MVP6378R: GAT TCA GGT CAG AAA GAG GTC ACA for the villin-cre transgene. Throughout the study animals were maintained on a C57BL/6 background. All animals were housed in microisolater polycarbonate cages in non-barrier mouse rooms (conventional housing). The procedures used in this study were approved by the University of Michigan Animal Care and Use Committee.

Histological analysis

Adult mouse intestine, kidney, liver, lung, spleen and stomach were fixed in 4% formaldehyde, dehydrated and embedded in paraffin. Sections (4 _M) were stained with hematoxylin and eosin (H&E). Sections were also immunostained overnight with polyclonal ZBP-89 antibody at a working dilution of 1:200 and counterstained with DAPI (44). Alkaline Phosphatase staining was performed on sections according to the manufacturer's suggestions using the Vector Red Alkaline Phosphatase Substrate Kit 1 from Vector Laboratories, Burlingame, CA. Goblet cells in the intestine were visualized by Alcian Blue staining (Dako, Carpinteria, CA). Sections were also immunostained for Chromogranin A (Abcam, Cambridge, UK), the Paneth cell marker Cryptdin, and BrdU.

RT-PCR analysis of ZBP-89 expression

Total cellular RNA was isolated from mouse lung and intestine using TRIzol Reagent (Invitrogen, Carlsbad, CA). Samples underwent DNase1 treatment (Invitrogen) before cDNA synthesis using iScript cDNA Synthesis Kit (Bio-Rad Laboratories, Hercules, CA). QRT-PCR was performed using Platinum Taq DNA Polymerase (Invitrogen). Mouse primer sequences (5' to 3') included: Ex6-F: GGC ATG TCT TCA TTC ATA GAG G and Ex8-R: CTC ATA CCA CAT TCA TCA CAG C for ZBP-89; CgA-F: AAG AAG AGG AGG AGG AAG AGG and CgA-R: TCC ATC CAC TGC CTG AGA G for Chromogranin A; GAPDHT-F: TCA AGA AGG TGG TGA AGC AGG and GAPDHT-R: TAT TAT GGG GGT CTG GGA TGG for GAPDH; Hes1-F: GCT CAC T C GGA CTC CAT GTG and Hes1-R: GCT AGG GAC TTT

ACG GGT AGC A for Hes1; Lyz-F: ATG GAA TGG CTG GCT ACT ATG and Lyz-R: CTC ACC ACC CTC TTT GCA CAT TG for Lysozyme; Muc2-F: AGA ACG ATG CCT ACA CCA AG and Muc2-R: CAT TGA AGT CCC CGC AGA G for Muc2; Ngn3-F: ACC CTA TCC ACT GCT GCT TGT C and Ngn3-R: CGG GAA AAG GTT GTT GTG TCT CTG for Ngn3; Math1CDS-F: GCC TTG CCG GAC TCG CTT CTC and Math1CDS-R: TCT GTG CCA TCA TCG CTG TTA GGG for Math1; TFF3-F: TTG CTG GGT CCT CTG GGA TA and TFF3-R: GCC GGC ACC ATA CAT TGG for TFF3; CryptdinQPCR-F: AGG AGC AGC CAG GAG AAG and CryptdinQPCR-R: ATG TTC AGC GAC AGC AGA G for Cryptdin; SM22a-F: CTC TAA TGG CTT TGG GCA GTT TGG and SM22a-R: GCT CCT GGG CTT TCT TCA TAA ACC for smooth muscle actin alpha.

Results

Generation of intestinal floxed ZBP-89 mice (ZBP-89$^{\Delta INT}$)

ZBP-89 FLP mice were previously generated and maintained on a C57BL/6 background. In these mice, intron 7 of the ZBP-89 gene contained a loxP site as well as a FRT site. A subsequent loxP site was located downstream of the translational stop codon of exon 9 (Figure 3-1A). In the presence of Cre recombinase, recombination occurs between the loxP sites leaving a single loxP site remaining in the locus after exons 8 and 9 were deleted (Figure 3-1A). Heterozygous mice (ZBP-89$^{FLP/+}$) were bred to mice expressing Cre recombinase under the control of 12.4 kb of the mouse villin promoter (28). The resulting heterozygous animals positive for the villin-cre transgene were bred together to

generate homozygous mice. PCR-based genotyping using primers specific for ZBP-89 and the villin-cre transgene confirmed generation of all possible genotypes (Figure 3-2B). Mouse growth recorded from weaning (3 weeks of age) until 12 weeks of age showed a trend towards smaller floxed mice compared to wild-type littermates, however this difference was not significant (p-value = 0.067) (Figure 3-1C). Homozygous floxed mice 12 weeks of age were not available for growth analysis as they had already been euthanized for other portions of this study.

Changes in intestinal morphology in ZBP-89^{-INT}

Upon tissue dissection from floxed mice, there were no gross abnormalities in the majority of the tissues examined. However, the mucosa of the intestine appeared thicker with eminently pronounced Peyer's patches in the homozygous floxed mice. There are several cell types that populate the intestinal epithelium and given the number of regulatory pathways involved in generating this characteristic pattern, we determined if floxed mice showed changes in these cell populations (Figure 3-2A). Hematoxylin and eosin (H&E) stain showed no abnormalities in wild-type villin-cre positive tissues (Figure 3-2B). Heterozygous floxed intestine showed a slight increase in goblet cell number but no other obvious changes (Figure 3-2C). On the other hand homozygous floxed mice showed dramatic increases in goblet and Paneth cells (Figure 3-2D). Some of these mice also demonstrated complete loss of villi throughout much of the small intestine. In addition the muscle layer surrounding the intestine was expanded in homozygous mice even though the villin promoter is only active in the epithelium. The variability in intestinal morphology could be due to incomplete ZBP-89 deletion as a result of patchy villin-cre

expression. Patchy expression in both the intestine and colon upon crossing mice carrying the villin-cre transgene with Rosa26 mice has been observed (Deborah Gumucio, personal communication).

Reduced epithelial proliferation in ZBP-89$^{\Delta INT}$

Two hours prior to dissection, mice were injected intraperitonally with the proliferation marker BrdU. It was expected that this marker would be incorporated into intestinal crypt cells (and not cells in the villi themselves) where the intestinal stem cell niche resides (5, 18, 41). Previously, the stem cell niche was thought to be only at the +4 position from the base of the crypt. However, recent evidence also suggests cells with stem-like properties reside at the very base of the crypt (5). Wild-type mice successfully incorporated the label into both cells at the base as well as cell on the sides of the crypt (Figure 3-3A). This pattern is also mimicked in the heterozygous floxed mice (Figure 3-3B). Homozygous floxed mice show less overall proliferation as defined through BrdU incorporation; most interesting is the loss of positive cells in the very base of the crypt (Figure 3-3C).

Reduced ZBP-89 staining and expression in the intestine

To confirm ZBP-89 deletion or reduction in the intestine, sections were stained using a rabbit ZBP-89 antibody (32). While ZBP-89 is a transcription factor, staining demonstrated both cytoplasmic and nuclear immunofluorescence in wild-type mice with higher expression in the epithelium (Figure 3-4A). Heterozygous floxed mice show reduced immunofluorescence throughout the epithelium (Figure 3-4B). Homozygous floxed mice show varying amounts of ZBP-89 reduction by this

method, perhaps due to mosaic expression of Cre recombinase (Figure 3-4C). QPCR quantitation confirmed a reduction in ZBP-89 mRNA levels in homozygous floxed animals, however this was not statistically significant (P = 0.718) (Figure 3-4D). This slight reduction is likely the result of whole tissue being utilized for mRNA and not specifically the epithelium where ZBP-89 is deleted.

Expansion of Paneth and goblet cell lineages in ZBP-89$^{\Delta INT}$

The secretory lineage forms three distinct cell types in the intestine, including: enteroendocrine cells, goblet cells and Paneth cells, which secrete hormones, mucous, and antimicrobial peptides respectively. Immunostaining for the pan-endocrine marker Chromogranin A (CgA) showed no change in the overall number of CgA positive cells between wild-type and floxed mice (Figure 3-6). This was also confirmed by QPCR using specific primers for CgA to examine message levels in the small intestine, suggesting endocrine cells are not altered by the loss of ZBP-89 (Figure 3-7C). However, the distribution of CgA positive cells was altered. Normally endocrine cells appear singly in the intestinal epithelium and are not in close proximity as a result of Notch-mediated lateral inhibition (8). Endocrine cells were frequently clustered in homozygous floxed mice, suggesting that loss of ZBP-89 altered the lateral inhibition process that orchestrates the normal pattern of secretory cell distribution. On the other hand immunostaining for the Paneth cell marker, cryptdin, showed a marked increase in this cell population between homozygous floxed and wild-type mice (Figure 3-5D, E, F). Consistent with increased Paneth cell immunostaining, expression of the Paneth cell marker lysozyme was increased in floxed mice (Figure 3-7B). This increase was 2.6-fold (P = 0.012) in homozygous

floxed mice compared to wild-type. From the H&E analysis it was obvious that goblet cells were increased in number. To formally demonstrate this increase, goblet cells were visualized by PAS/alcian blue staining (Figure 3-5A, B, C). Indeed heterozygous floxed mice show a slight increase in goblet cell number and those homozygous for ZBP-89 deletion demonstrate a marked increase. Analysis of mRNA expression of the goblet cell marker Muc2, however, showed a trend towards increased expression levels but this was not statistically significant (Figure 3-7A). Given the apparent elevation detected by immunohistochemistry, it is possible that analysis of more mice will generate significance in the differences observed between genotypes.

Reduced absorptive lineage in homozygous ZBP-89$^{\Delta INT}$

To test whether the expansion of secretory cells affected the differentiation of the absorptive lineage, we examined enterocyte numbers in the floxed mice. Immunohistochemistry staining of enterocytes by alkaline phosphatase showed normal cell numbers in the wild-type and heterozygous mice. However, ZBP-89$^{\Delta INT}$ mice resulted in reduced numbers of alkaline phosphatase positive cells (Figure 3-8A-C). Several mice demonstrated complete loss of this lineage, whereas, several others showed complete loss at the base of villi but positive staining near the villus tip (Figure 3-8C). This phenotype variance could be the result of patchy Cre expression in a subset of mice leading to incomplete loss of ZBP-89.

Discussion

While previous studies have failed to obtain viable ZBP-89 knock-out animals, we report here the successful gene targeting and tissue specific deletion of ZBP-89 in the mouse small intestine. Through this process we have avoided complications observed in other models of ZBP-89 deletion, such as the failure of male germ cell development and disruption of both primitive and definitive hematopoiesis (25, 43). Furthermore, mice deficient in ZBP-89 throughout the intestinal epithelium are not only viable, but survive through at least 2 months of age without lethal complications. Mice homozygous for Cre mediated deletion demonstrate growth reduction as determined by body weight from weaning through adulthood. While the change in body weight was not significant in the sample size currently used, it was probable that with more mice observed over the entire 12-weeks of data collection significance might be obtained. This alteration in body weight is also expected given the dramatic loss in nutrient absorbing enterocytes in the floxed mice. Over time these mice may experience severe complications and wasting as a result of the lack of enterocytes.

Studies with mutant mouse strains indicating that intestinal crypts are monoclonal in nature support the existence of intestinal stem cells (ISCs) (7, 17, 40). As is the definition for other types of stem cells, ISCs are defined as cells that replenish themselves through self-renewal and also give rise to all of the cell types found in the intestinal epithelium. Thusly, under normal conditions, an ISC divides asymmetrically, giving rise to 2 daughter cells, 1 stem cell and 1 committed cell which will then differentiate. While it is known that ISCs reside in the intestinal

crypts, the exact location and defining markers of these cells are highly speculative. The most widely accepted theory defines ISCs as long-term label retaining cells (LRCs), an average of 4 cells up from the crypt base (29, 37). It is important to note that crypts form a ring structure with roughly 16 cells occupying the +4 position, however only 4-6 ISCs are thought to reside in a single crypt (7). In a 2007 study by Barker and colleagues, lineage tracing experiments were utilized to identify crypt base columnar cells (CBCs) positive for the marker Lgr5/GPR49 as possible ISCs (5). These cells were shown to reside in the crypt base between Paneth cells and are capable of self-renewal, multipotent for all mature intestinal epithelial cells and persist over a 60-day period (5). It is possible that both stem cell theories are indeed correct and reflect the many underlying signaling pathways that play a role in regulating cells of the intestinal epithelium, such as Wnt, Notch, and BMP. In point of fact, Linheng Li and coworkers recently reported that like skin, there are 2 stem cell niches one at +4 (LRC) and one in the crypt base columnar cells (CBC) (41). Mice homozygous for intestinal epithelial ZBP-89 deletion appear devoid of proliferating cells normally found in the crypt base, presumably Lgr5 + CBCs. Further studies will be performed to determine if indeed these cells are missing upon ZBP-89 deletion. However this is quite interesting given the changes seen in absorptive and secretory lineage cell populations. It is possible that normally +4 LRCs generate cells of the secretory lineage and it is known that Lgr5+ cells are capable of regenerating all of the epithelial cell types. Therefore if loss of ZBP-89 leads to loss of Lgr5+ ISCs, the remaining +4 LRCs may be capable of regenerating all intestinal epithelial cells except the enterocytes, accounting for the loss of CBCs

and replacement with the differentiated secretory lineages goblet/Paneth cells in the ZBP-89$^{\Delta INT/\Delta INT}$ mice.

Goblet, enteroendocrine and Paneth cells all are thought to arise from a single secretory progenitor cell. In ZBP-89 floxed mice it appears that only goblet and Paneth cells are affected and not all secretory cells. This places ZBP-89 downstream of the secretory cell specific transcription factor Math1, since mice containing a Math1 null mutation exhibit loss of all endocrine, goblet, and Paneth cell markers (50). Interestingly, Math1 gene expression is upregulated in floxed mice presumably due to the loss of enterocytes and a driving force towards secretory lineages (data not shown). Recent evidence suggests a bipotential secretory progenitor exists, capable of differentiating into either endocrine precursors or goblet and Paneth cell precursors (26). Given that enteroendocrine cells do not appear altered by the loss of ZBP-89, I predict that this factor plays a role in goblet and Paneth cell differentiation downstream of this bipotential secretory progenitor. However, given that ZBP-89 is normally ubiquitously expressed and the large number of known interacting proteins and signaling pathways, it is likely that loss of ZBP-89 is affecting a number of pathways to yield the observed phenotype.

In the intestinal epithelium Wnt signals are known to be involved in maintaining stem/progenitor cells via cell cycle control, directing secretory lineage development, and controlling localization and migration of cells along the crypt-villus axis (10). A gradient of active Wnt signaling occurs in the crypt where signaling is greatest in Paneth cells and cells in positions 2-6 (where ISCs are thought to be located), whereas signaling is less active in positions 6 and above in the crypt (13).

While it is well known that the Wnt pathway plays a role in early secretory development, it has also been shown to have divergent effects on the maturation of specific secretory cell types. Specifically, Wnt signaling is critical for Paneth and goblet cell development, but is not required for maturation of enteroendocrine cells (45, 47). Upon deletion of the Wnt dependent gene Sox9, mice display a complete lack of Paneth cells, which lead the authors to conclude that this gene is a critical component of the Wnt pathway required for Paneth cell maturation (6, 34). In addition, Sox9 knock-out mice also display a reduction in goblet cells suggesting that this factor plays a role in at least 2 secretory lineages (6). ZBP-89 may normally play a role interacting with a number of factors in the Wnt pathway. In fact, an interaction with Sox9 is perhaps quite probable. Given the goblet and Paneth cell phenotype of floxed ZBP-89 mice and the striking connection with Sox9's involvement in the development of these cell types, an interaction should be further pursued. ZBP-89 has been shown to interact with both Sox14 and Sox18 by *in vitro* methods, and Sox4 was identified a microarray using cells depleted of ZBP-89 (Bai and Merchant unpublished results) (12, 36). Interestingly Sox4 is a known target of Wnt signaling and is thought to function through stabilizing the β-catenin protein (38, 42). In a study of Apc^{Min} adenomas and colorectal cancer cell lines, Sox4 expression was strongly increased (38). Therefore confirming an interaction between Sox4 and ZBP-89 could firmly place ZBP-89 as an inhibitor of the Wnt signaling pathway.

The transcription factor ZBP-89 is associated with signaling pathways involved in embryogenesis, cellular proliferation, differentiation, growth arrest and

apoptosis. For this reason, conditional deletion in any tissue is likely to have multiple outcomes not solely attributable to disruption of any one pathway. In the intestine, deletion of ZBP-89 results in increased numbers of goblet and Paneth cells, loss of enterocytes and reduced crypt proliferation. Defining a mechanism for this observed phenotype is likely to involve ZBP-89's disruption of more than one developmental event (Figure 3-9). Future studies should focus on ZBP-89 in Lgr5+ ISCs as well as ZBP-89's involvement with the Wnt signaling pathway.

Acknowledgements

The authors thank Lisa Travnikar, Gayan DeSilva, Dan Kechele and Kelli VanDussen for technical assistance. The authors gratefully acknowledge the expertise of the University of Michigan Transgenic Animal Model Core, especially Thom Saunders, Linda Samuelson and Elizabeth Hughes. The authors would also like to thank Deborah Gumucio and Kathy Portman for the villin-cre mice, and the Unit for Laboratory Animal Medicine at the University of Michigan.

Figure 3-1. Intestinal deletion of ZBP-89 results in viable animals. **A.** Schematic representation of targeted locus. Single loxP (L) and FRT (F) sites are located upstream of ZBP-89 exon 8 while a second loxP site is downstream of exon 9. Upon expression of CRE recombinase driven by the intestinal specific villin promoter cre mediated excision occurs leaving a single loxP site in place of exons 8 and 9 of ZBP-89. **B.** Genotyping of targeted mice demonstrates a wild-type ZBP-89 fragment 596 bp and a ZBP-89 FLP fragment of 674 bp (top panel), genotyping for the villin-cre allele shows an 881 bp fragment corresponding to villin and a 350 bp fragment which corresponds to CRE (bottom panel). Lane 1 ZBP-89 FLP/FLP villin-cre +, lane 2 ZBP-89 FLP/+ villin-cre +, lane 3 wild-type villin-cre +. **C.** Growth chart displaying mouse weight (g) from weaning through 12 weeks of age. Each data point represents an average of 5 animals. Differences are not statistically significant at any time point.

A.

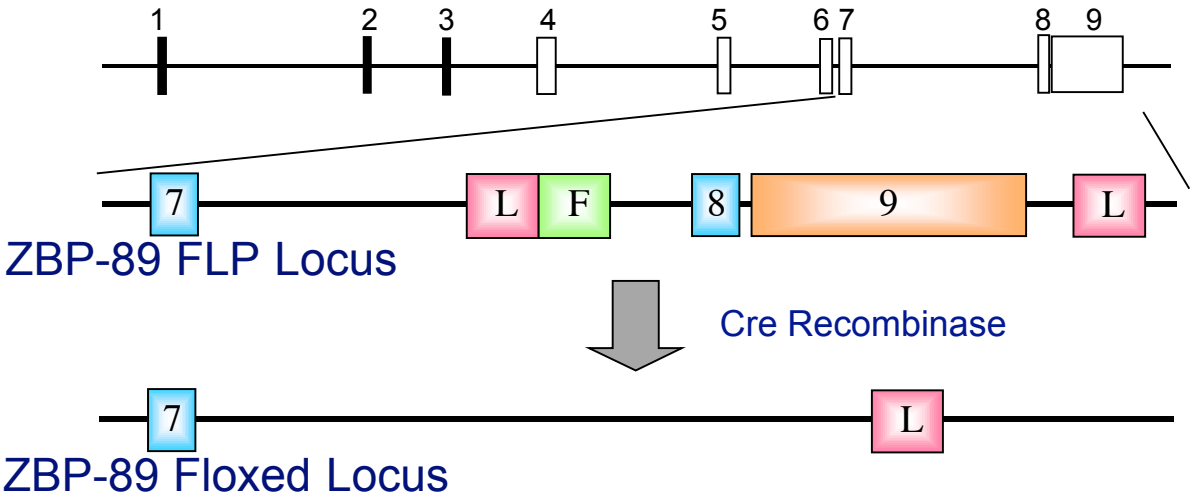
1
2
3
4
5
6 7
8
9
7
L
F
8
9
L
ZBP-89 FLP Locus
Cre Recombinase
7
L
ZBP-89 Floxed Locus

B.

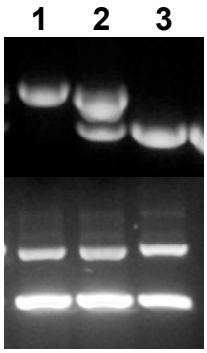
1
2
3

C.

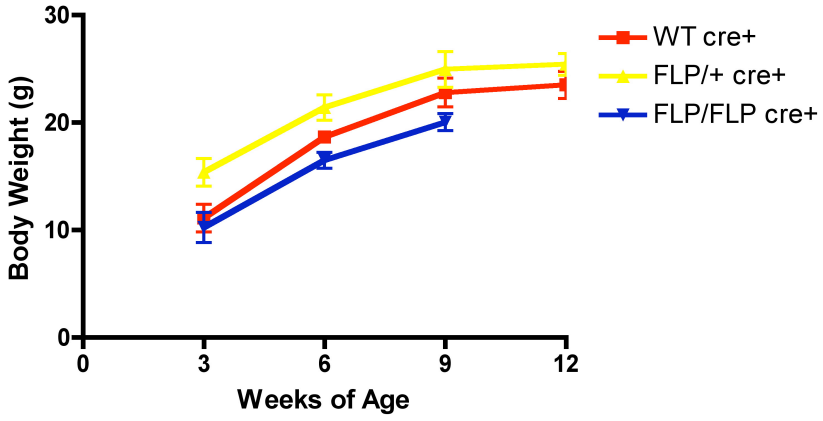
30
20
10
0
Body Weight (g)
0
3
6
9
12
Weeks of Age
WT cre+
FLP/+ cre+
FLP/FLP cre+

Figure 3-2. Deletion of the ZBP-89 locus in the small intestine results in both epithelial and mesenchymal alterations. **A.** An enlarged view of a villus and its corresponding crypt in the small intestine depicting the cell types that populate this area. **B – D.** H&E stained sections of mouse duodenum. Black arrows indicate goblet cells lining villi epithelium, blue arrows indicate to the muscle layer. All sections are 200X. **B.** Wild-type villin-cre+ **C.** ZBP-89 FLP/+ villin-cre+ **D.** ZBP-89 FLP/FLP villin-cre+.

A.

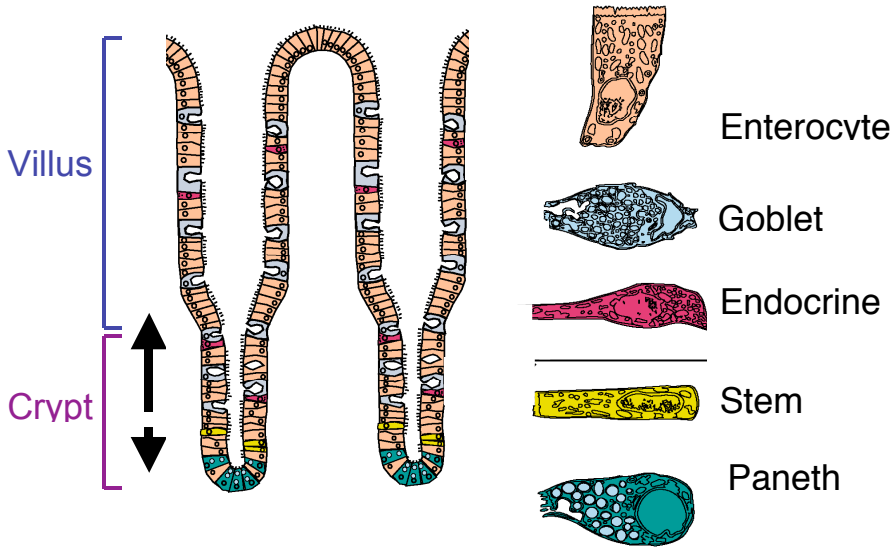

B.

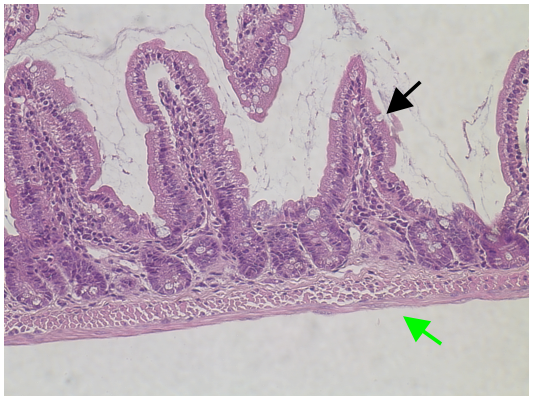

C.

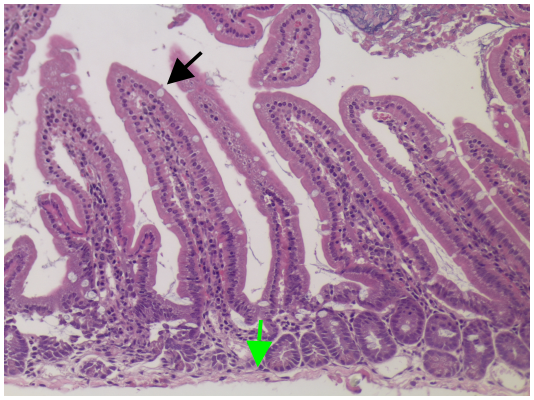

D.

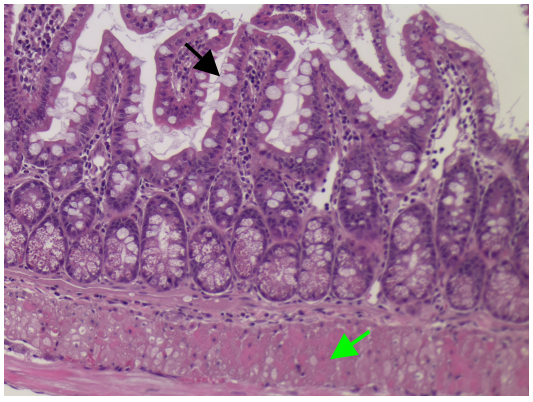

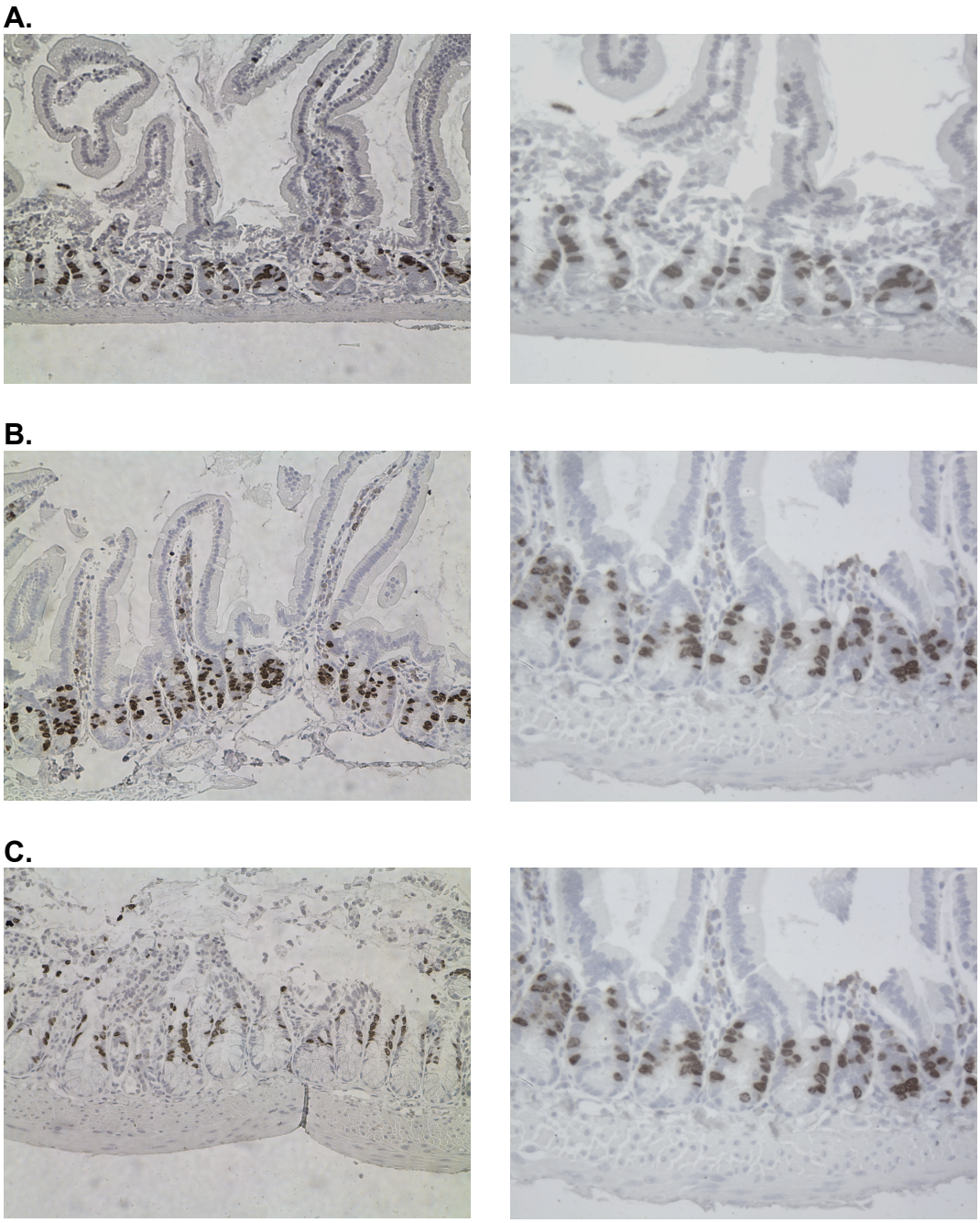

Figure 3-3. Incorporation of the proliferation marker BrdU in the small intestine. **A.** Wild-type. **B.** ZBP-89 FLP/+ villin-cre +. **C.** ZBP-89 FLP/FLP villin-cre +. Left panel is 200X magnification while right panel is 400X.

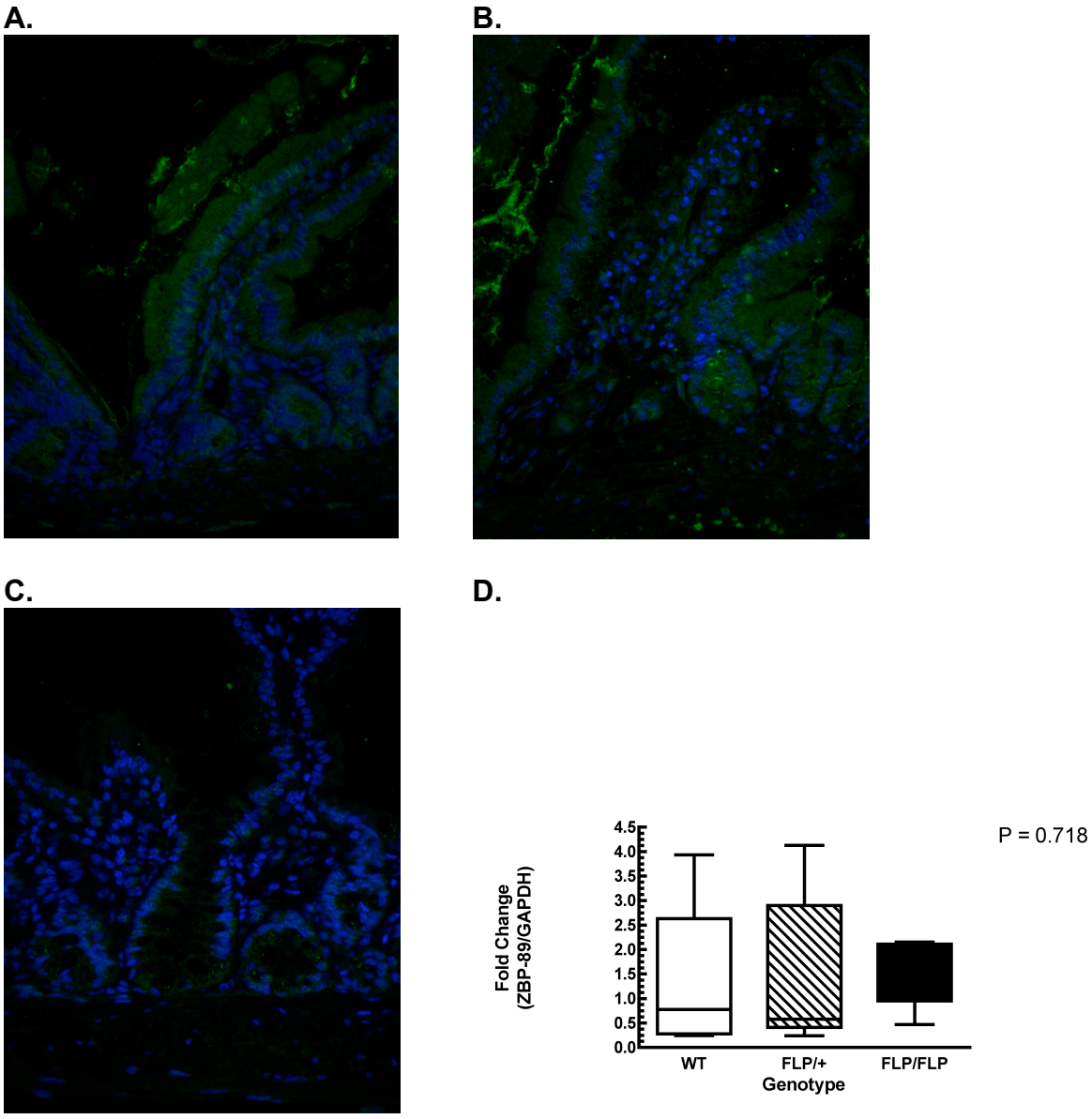

Figure 3-4. ZBP-89 expression in the mouse duodenum. **A.** Wild-type. **B.** ZBP-89 FLP/+ villin-cre +. **C.** ZBP-89 FLP/FLP villin-cre +. Panels show merged images of ZBP-89 (FITC) with DAPI nuclei counterstain. All sections are 200X. **D.** QPCR analyses ZBP-89 expression. Data shown were generated from 5 mice per genotype with each sample performed in triplicate.

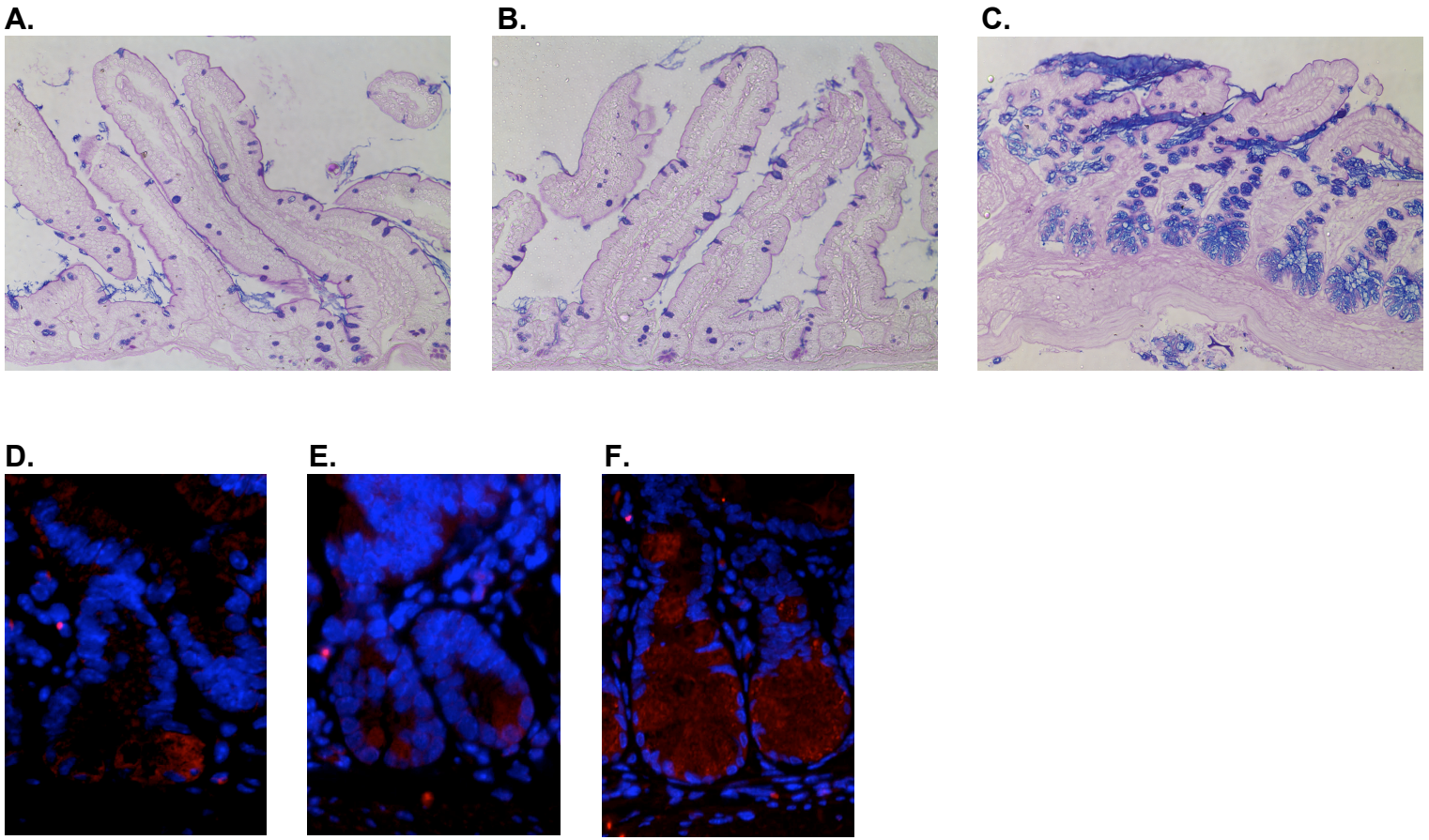

Figure 3-5. Identification of intestinal goblet and Paneth cells. **A - C.** PAS/Alcian Blue immunohistochemistry of goblet cells (blue). **D - F.** Cryptdin immunofluorescence of Paneth cells (red), DAPI counterstain of nuclei. **A, D.** Wild-type. **B, E.** ZBP-89 FLP/+ villin-cre +. **C, F.** ZBP-89 FLP/FLP villin-cre +.